Journal for ImmunoTherapy of Cancer

Neoadjuvant personalized viral vaccine prevents tumor relapse in checkpoint-resistant murine melanoma model

Laura Seclì , Linda Nocchi , Guido Leoni, Gabriella Cotugno, Fulvia Troise , Giuseppina Romano, Teresa Busiello , Elisa Micarelli, Irene Garzia, Laura Antonucci, Elisa Scarselli , Anna Morena D'Alise

To cite: Seclì L, Nocchi L, Leoni G, *et al*. Neoadjuvant personalized viral vaccine prevents tumor relapse in checkpoint-resistant murine melanoma model. *Journal for ImmunoTherapy of Cancer* 2025;**13**:e013035. doi:10.1136/jitc-2025-013035

► Additional supplemental material is published online only. To view, please visit the journal online (https://doi.org/10.1136/jitc-2025-013035).

Accepted 17 November 2025

NousCom Srl, Rome, Lazio, Italy

Correspondence to
Dr Anna Morena D'Alise;
m.dalise@nouscom.com

ABSTRACT

Background Personalized cancer vaccines targeting tumor-specific neoantigens (nAgs) are an emerging therapeutic strategy, particularly effective in early-stage disease before immune suppression is established. Immune checkpoint inhibitors have demonstrated benefit in the adjuvant setting (postsurgery), and recent evidence suggests neoadjuvant administration (before surgery) may further enhance antitumor immunity. This study evaluated the efficacy of a multiepitope nAg vaccine in a preclinical melanoma model resistant to checkpoint inhibition, comparing neoadjuvant and adjuvant treatment, alone or in combination with anti-programmed cell death protein 1 (PD1) therapy.

Methods A viral vector nAg vaccine was developed and administered in the B16F10 murine melanoma model. Mice received the vaccine either before (neoadjuvant) or after (adjuvant) tumor resection alone or in combination with anti-PD1. Tumor recurrence and survival were assessed. Immune profiling was performed to evaluate T cell phenotypes, and $CD8^+$ T cell depletion experiments were conducted to assess the role of this population. Protection against tumor rechallenge was considered to evaluate long-term immunity.

Results Neoadjuvant vaccination alone provided approximately 70% protection against tumor recurrence. When combined with anti-PD1, protection increased to 90%. Notably, anti-PD1 alone conferred 60% protection when used in a neoadjuvant setting. In contrast, adjuvant vaccination was ineffective as monotherapy and required combination with anti-PD1 to prevent relapse. The efficacy of neoadjuvant vaccination was dependent on $CD8^+$ T cells and associated with robust effector memory T cell responses. Long-term protection against tumor rechallenge was superior in the neoadjuvant vaccine group compared with anti-PD1 alone.

Conclusions Neoadjuvant nAg vaccination elicits potent $CD8^+$ T cell-mediated immunity and offers superior protection against tumor recurrence and rechallenge compared with adjuvant approaches or checkpoint blockade alone. These findings support the clinical evaluation of neoadjuvant cancer vaccines, particularly in settings where tumors are resistant to conventional immunotherapy.

WHAT IS ALREADY KNOWN ON THIS TOPIC

⇒ Surgical resection is the primary treatment for many solid tumors, yet recurrence and metastatic progression remain frequent, underscoring the need for effective perioperative therapies. Immunotherapy has reshaped cancer care, demonstrating durable benefit in multiple malignancies. Among novel approaches, personalized cancer vaccines targeting tumor-specific neoantigens (nAgs) represent a promising strategy, particularly when administered in early-stage disease prior to the establishment of immune suppression. In the adjuvant setting (postsurgery), recent clinical studies have reported encouraging outcomes, including improved recurrence-free survival and a strong correlation between vaccine-induced T cell expansion and clinical benefit across tumor types. Immune checkpoint inhibitors (CPIs) have already demonstrated a clinical advantage in the adjuvant context, and emerging evidence indicates that neoadjuvant administration may further potentiate antitumor immunity, supporting investigation of cancer vaccines in this earlier setting.

BACKGROUND

Immunotherapy has transformed the landscape of cancer treatment, offering significant clinical benefits in several malignancies. However, only a subset of patients experiences durable responses, highlighting the need for strategies that broaden its therapeutic effect. Integrating immunotherapy with established treatment modalities, particularly surgery, is emerging as a promising approach to improve outcomes. For many solid tumors, surgery remains the primary treatment; however, resection alone is not always curative, due to local relapse and metastases spreading. Therefore, immunotherapy administration, either in neoadjuvant (presurgery) or adjuvant (postsurgery) setting, has the potential to enhance long-term survival by targeting residual disease and reducing the risk of recurrence.[1] Checkpoint inhibitors (CPIs)

WHAT THIS STUDY ADDS

⇒ This is the first study demonstrating the superior efficacy of a nAg-based vaccination as monotherapy in neoadjuvant over adjuvant setting, in the CPI-resistant preclinical model of B16F10, achieving the best therapeutic response and the highest rate of protection from relapse when it is combined with anti-programmed cell death protein 1 (PD1). Neoadjuvant vaccination, but not neoadjuvant anti-PD1 therapy alone, is able to generate durable immunity that protects mice from tumor recurrence and metastasis. This approach expands antigen-specific T cells with a memory phenotype that persist in the periphery long after surgical tumor removal and induces a high infiltration of $CD8^+$ T cells into both the tumor and tumor-draining lymph nodes. These $CD8^+$ T cells exhibit a less-exhausted, more "stem-like" phenotype, indicative of enhanced antitumor effector function. Together, these findings support the concept that neoadjuvant vaccination establishes a functional antitumor immune memory capable of providing long-term protection against tumor recurrence.

HOW THIS STUDY MIGHT AFFECT RESEARCH, PRACTICE OR POLICY

⇒ This study provides compelling preclinical evidence that neoadjuvant administration of personalized cancer vaccines may offer superior therapeutic benefit compared with adjuvant use. In both adjuvant and neoadjuvant settings, combination of vaccine with anti-PD1 has superior therapeutic efficacy at reducing tumor recurrence/relapse than anti-PD1 alone. This data suggests that employing nAg vaccination as part of combination immunotherapy alongside checkpoint blockade is a highly promising therapeutic approach. Continued progress in manufacturing technologies, together with the supportive data generated by studies such as ours, could make this strategy both feasible and impactful and may open a new avenue in cancer immunotherapy, informing future clinical trial design and guiding the integration of personalized vaccines into perioperative treatment paradigms.

in the adjuvant setting have already demonstrated the ability to prolong recurrence-free survival, particularly in patients with CPI-responsive indications like melanoma and non-small cell lung cancer. Despite these advances, a substantial proportion of patients who receive adjuvant CPIs eventually relapse, suggesting that additional strategies are needed to maximize their effectiveness.[2–4]

One promising approach involves the use of personalized cancer vaccines targeting tumor neoantigens (nAgs). These vaccines are designed to elicit potent antitumor immunity, especially in conditions of minimal residual disease, for example after surgery. Preclinical studies have shown that while cancer vaccines as standalone treatment demonstrate limited efficacy against large, established tumors—likely due to the immunosuppressive tumor microenvironment—combining them with CPIs can significantly enhance the therapeutic outcomes.[5–8]

Recent clinical data support the promise of this approach, in several tumor indications. A randomized Phase II trial of a personalized messenger RNA vaccine combined with pembrolizumab in patients with resected high-risk melanoma showed that the combination therapy significantly prolonged recurrence-free survival versus pembrolizumab monotherapy.[9] Moreover, a Phase I trial exploring the efficacy of adjuvant individualized nAg vaccine in combination with anti-programmed death-ligand 1 and chemotherapy in patients with resected pancreatic ductal adenocarcinoma showed encouraging preliminary clinical benefits, with a positive correlation between vaccine-induced nAg-specific immunity and recurrence-free survival at 3.2-year follow-up.[10 11] A second Phase I clinical trial of a peptide-based nAg personalized cancer vaccine in high-risk fully resected clear cell renal cell carcinoma with or without anti-CTLA4 ipilimumab showed absence of recurrence in all nine vaccinated patients, along with immune responses against vaccine-targeted nAgs and durable expansion of peripheral T-cell clones.[12]

An alternative and potentially more effective strategy is the administration of immunotherapy in the neoadjuvant setting, before tumor removal. Preclinical and early clinical evidences suggest that neoadjuvant immunotherapy can be more effective than adjuvant treatment across several malignancies, enhancing antitumor immune responses and improving long-term survival.[1 13] By initiating immunological priming while the primary tumor is still present, neoadjuvant immunotherapy stimulates a more robust immune response that may help to prevent relapse.[14 15] Neoadjuvant immunotherapy-based clinical trials have provided further validation of this approach. For instance, a recent Phase III trial in resectable stage III melanoma demonstrated that presurgical CPI administration resulted in significantly longer disease-free survival compared with postsurgical adjuvant treatment.[16–18] The superior efficacy of neoadjuvant immunotherapy appears to be driven by several factors, including the reduction of tumor burden prior to surgery, increased breadth and durability of tumor-specific T cell responses, and the presence of effector and memory T cells in the tumor-draining lymph nodes (tdLNs), which may prevent recurrence and target micrometastases.[14 16 19]

In this study, we investigated the therapeutic effectiveness of a multiepitope Great-Ape Adenoviral (GAd) vaccine targeting B16F10 nAgs in neoadjuvant (prior to surgery) and adjuvant (after surgery) settings, alone or in combination with anti-programmed cell death protein 1 (PD1). We demonstrated that, when administered in a neoadjuvant setting, vaccination was effective as a standalone treatment and achieved the highest efficacy with the lowest relapse rate when combined with anti-PD1.

These findings underscore the potential of neoadjuvant vaccination to reduce tumor recurrence and improve patient outcomes, offering a compelling rationale for further exploration of this approach in clinical settings.

METHODS

Cell cultures

B16F10 (murine C57BL/6 melanoma), CT26 (murine BALB/c colorectal carcinoma), MC38 (murine C57BL/6 colon adenocarcinoma) and 4T1 (murine BALB/c breast

cancer) cell lines were purchased from American Type Culture Collection. B16F10 and MC38 cells were maintained in Dulbecco's Modified Eagle Medium (Gibco, cat. 41966052); CT26 and 4T1 cells were cultured in RPMI 1640 (Gibco, cat. 21875091). Media was supplemented with 10% heat-inactivated fetal bovine serum (FBS) (Gibco, cat. A5670701), 1% (v/v) penicillin/streptomycin (Gibco, cat. 15140122) and 2 mM L-Glutamine (Gibco, cat. 25030024). Cells were maintained at 37°C in 5% CO_2 and routinely tested for mycoplasma contamination by PCR.

Exome and RNA sequencing of murine tumors

DNA and RNA library construction and NGS of B16F10 tumor samples were performed at CeGaT GBMH (Tübingen, Germany). Genomic DNA was fragmented and used for Illumina library construction. Exonic regions were captured in solution using the Twist Mouse Exome kit (Twist Biosciences). Paired-end sequencing (2×100 bp) was performed with the NovaSeq 6000 sequencer (Illumina, San Diego, California, USA) by requiring a target depth of coverage of at least 30 Gb. RNA was fragmented and the sequencing library was prepared using the SMART-Seq stranded kit (Takara). Sequencing was performed with the NovaSeq 6000 sequencer (Illumina) at a target depth of coverage of 60 million read pairs (2×100 bp). Germline sequence data of the C57BL/6 murine strain were downloaded from Sequence Read Archive (SRA) (experiment id: SRR10043182) and used as normal control sample.

A preliminary quality control of the raw sequence data was performed by filtering out reads of low quality with Trimmomatic-0.33. The remaining DNA and RNA read pairs were then aligned against the mm10 mouse reference genome using BWA-mem and hisat2, respectively. Read pairs for which only one read is mapped and paired reads that align to more than one genomic locus with the same mapping score were filtered out. Exomeseq alignments were then further processed by optimizing the local alignment around small indels, marking duplicated reads and recalibrating the final base quality score in the realigned regions (program, parameters) with Picard tools (http://broadinstitute.github.io/picard/ (V.2.20)). Somatic variant calling of single nucleotide variants (SNVs) and indels was performed on the recalibrated DNA read data using mutect2 and Varscan2 by explicitly comparing the tumor DNA data versus the normal control DNA data. SNVs that generate a non-synonymous (missense) change within a codon in the coding sequence (CDS) of protein-coding genes, identified by at least one variant caller, were retained. The initial list of SNVs was then further reduced by selecting only mutations that fulfill the following criteria: (1) mutation allele frequency (MAF) in the tumor DNA sample ≥10%; (2) ratio of the MAF in the tumor DNA sample and in the control DNA sample ≥5; (3) number of mutated reads at chromosomal position of somatic variant in the tumor DNA >2; (4) number of mutated reads at chromosomal position of somatic variant in the normal DNA <2. Each somatic variant was then translated into a peptide containing the mutated amino acid in order to predict binding of the putative nAg to the mouse C57BL/6 major histocompatibility complex (MHC) class-I alleles. nAg peptides were generated as 25-mer peptides with the mutated amino acid flanked upstream and downstream by 12 wild type (wt) amino acids. Gene expression estimates were performed using the Rsubsreads package and converting the raw counts estimated on refseq annotated genes, in transcripts for million. MHC-I binding predictions for 25-mer were performed by using the consensus method of the IEDB V.2.17 software considering the best predicted epitope comprising a non-wt amino acid.

Neoantigen selection

nAg selection was performed using a proprietary method, called VENUS (Vaccine-Encoded Neoantigens Unrestricted Selection), to prioritize mutated peptides with high potential to be nAgs.[20] This method assigns to each mutation a weighted score that combines the mutation allelic frequency, the abundance of the transcript coding for the mutation, and the likelihood to bind the class-I MHC alleles. All the detected mutated peptides encoded by mutations in B16F10 tumors were ranked and finally the top 62 ranked neopeptides were selected for the inclusion in the vaccine design.

Adenoviral vector production

GAd encoding nAgs selected from B16F10 was generated (GAd-B16F10), as previously described.[6 20] Briefly, the selected candidate nAgs were joined head to tail to generate an artificial polyepitope protein. The CDS for the transgene encoded in GAd (the corresponding amino acid sequences are listed in online supplemental table 1) was synthesized as phosphorylated gBlock dsDNA fragment (IDT). HA tags were added at the N- and C terminus of the transgene. The CDS was generated by Gibson assembly (New England Biolabs) and cloned into the respective shuttle plasmid containing the cytomegalovirus promoter with two TetO operator repeats and a BGH polyA. The expression cassettes were then transferred into pGAd plasmid, with the regions E1/E3/E4 deleted and E4 replaced with Ad5 E4 ORF6. The transgene was introduced in the E1 locus by homologous recombination in BJ5183 cells (Agilent). GAd vector was then produced by transfection of adherent M9 cells (293 cells derivative) with Lipofectamine 2000 (Invitrogen) and amplification in suspension M9 cells. Viral vector was then purified from infected cells by Vivapure Adenopack 20 RT (Sartorius). The titer was determined by quantitative PCR and expressed as viral particles (vp) per mL.

Mice

Daily animal care was performed by trained mouse house staff at Plaisant, Castel Romano. All experimental procedures were approved by the Italian Ministry of Health and have been done in accordance with the applicable Italian

laws (DLgs 26/2014), the Institutional Animal Care and Allevamenti Plaisant SRL. 6-week-old female C57BL/6 and BALB/c mice were purchased from Envigo and used in all experiments. The choice of using only female mice was based on consistency and to reduce variability due to hormonal cycles in mixed-sex cohorts. Although only one sex was studied, the immune mechanisms investigated are not known to be sex-specific, and the findings are expected to be relevant to both sexes.

In vivo tumor growth

For neoadjuvant/adjuvant experiments and for established tumor setting, 1×10^5 B16F10 or 5×10^5 B16F10 cells were subcutaneously (s.c.) injected into the back or in the flank of C57BL/6 mice, respectively. For the study of lung metastases, 1×10^5 B16F10 cells were injected in the tail vein (intravenously) of C57BL/6 mice. For the MC38 colon carcinoma model, 2×10^5 cells were s.c. injected into the flank of C57BL/6 mice. For the CT26 colon carcinoma model, 1×10^6 cells were s.c. injected into the flank of BALB/c mice. For the orthotopic 4T1 breast cancer model, 5×10^4 cells were injected into the fourth mammary gland of BALB/c mice. Tumor mass was measured every 3–4 days with a digital caliper, applying the formula: $0.5\times\text{length}\times\text{width}^2$, where the length is the longer dimension. Animals were then randomized based on their tumor size (tumor size average per group ~50–100 mm^3) and started to receive treatments based on the study. Animal survival was monitored daily for the entire experiment and mice were euthanized as soon as signs of distress or a tumor volume above 1000 mm^3 was reached.

Surgical tumor resection was performed when tumor volume was on average 400–600 mm^3. Incisions were closed with AutoClip System 0,9 cm (FST, cat. 12022-19). After 7 days from surgery clips were removed.

Lung metastases were checked on day 20 post-tumor cell inoculum. Lungs were perfused with India Ink 15% (American Mastertech Scientific, cat. STIIN25 EA), harvested and fixed in Fekete's solution (700 mL/L 100% ethanol, 32 mL/L 37% formalin, 40 mL/L glacial acetic acid, distilled water to 1 L). Metastatic nodules on the surface of the lungs were counted using a dissecting microscope. When nodules were too many to be counted, a value of 100 was given.

In vivo drug administration

Vaccines were administered bilaterally, via intramuscular injection in both quadriceps by delivering a volume of 50 µl per side at 5×10^8 vp in A195 formulation buffer (pH 7.4; 10 mM Trizma, 10 mM Histidine, 5% sucrose, 75 mM NaCl, 1 mM $MgCl_2$, 0.02% PS-80, 0.1 mM EDTA, 0.5% (v/v) ethanol).

Murine anti-PD1 (Bio X Cell, clone RMP114, cat. BE0146) was intraperitoneal (i.p.) administered at a 200 µg dose, twice. To deplete T cell subsets, anti-mCD4 (Bio X Cell, clone GK1.5, cat. BE0119) and anti-mCD8 (Bio X Cell, clone YTS 169.4, cat. BE0117) were administered i.p. at a dosage of 200 µg. Administration schedules are indicated in each figure.

Ex vivo immune analysis

Interferon-gamma (IFNγ) Enzyme-linked immunosorbent-spot (ELISpot) assay was performed on cell suspension of spleens. MultiScreen HTS plates (Millipore, cat. MSIPS4510) were coated with 10 µg/mL of anti-mouse IFNγ antibody (U-CyTech, cat. CT317-c) and incubated overnight at 4°C. After washing and blocking, splenocytes were plated in duplicate at two different cell densities (5×10^5 and 2.5×10^5 cells) and stimulated overnight with single 25-mer peptides or peptide pool (TEMA ricerca, matching the peptide sequences listed in online supplemental table 1) at a final concentration of 1 µg/mL. The peptide diluent dimethyl sulfoxide (DMSO, Sigma-Aldrich, cat. D2650) and Concanavalin A (Con A, Sigma-Aldrich, cat. C5275) were used as negative and positive controls, respectively. Plates were then incubated with biotinylated anti-mouse IFNγ antibody (dilution 1:100, U-CyTech, cat. CT317-c), conjugated streptavidin-alkaline phosphatase (dilution 1/2500, BD, cat. 554065) and 5-bromo-4-chloro-3-indoyl-phosphate/nitro blue tetrazolium 1-Step solution (Thermo Fisher Scientific, cat. 34042). An automated video analysis system was used to analyze the plates (CTL ImmunoSpot S6 Ultimate). ELISpot data were expressed as IFNγ spot forming colonies (SFCs) per million splenocytes. ELISpot responses were considered positive if all the following conditions occurred: (1) IFNγ production present in Con A stimulated wells, (2) the number of spots seen in positive wells was three times the number obtained in the negative control wells (DMSO), (3) at least 30 specific spots/million splenocytes. For IFNγ ELISpot post-$CD8^+$ T cell depletion, splenocytes were incubated with Dynabeads Mouse CD8 (Thermo Fisher Scientific, cat. 11 447D) following product instructions.

Tissue preparation and flow cytometry analysis

Tumors, spleens and tdLNs (brachial and axillary) were mechanically dissociated and then, depending on the tissue, enzymatically digested using Tumor Dissociation Kit (Miltenyi Biotech, cat. 130-096-730) for tumors, and Collagenase IV (0.2 mg/mL) in Hank's Balanced Salt Solution+2% FBS, for tdLNs. Tissue homogenates were then depleted from erythrocytes using Ammonium-Chloride-Potassium (ACK) Lysing Buffer (Gibco, cat. A1049201) and filtered through a 70 µm cell strainer to generate single-cell suspension ready for staining with markers of interest. Blood was collected at different time points after surgery in heparin-containing tubes, incubated with ACK buffer and filtered through 70 µm cell strainer, ready for staining.

For dextramer staining: isolated cells were stained with customized MHC-I-Ag complexes for AALTFRR-RL-PE (nAg1) or YGFRNVVHI-PE (nAg56) (Immudex), followed by incubation with the surface antibodies mix: Live/Dead Fixable Near-IR Dead Cell Stain Kit (Thermo Fisher Scientific, L10119); CD45 BV510 (clone 30-F11,

BioLegend; cat. 103138); CD8 PerCP-Cy5.5 (clone 53–6.7, BioLegend; cat. 100734); CD4 PE-Cy7 (clone RM4-5, BioLegend; cat. 100528). For effector memory (EM) ($CD8^+$ $CD44^+$ $CD62L^-$) and central memory (CM) ($CD8^+$ $CD44^+$ $CD62L^+$): Live/Dead Fixable Near-IR Dead Cell Stain Kit; CD8 BV510; CD44 APC (clone IM7, BioLegend; cat. 103012); CD62L FITC (clone MEL-14, BD; cat. 553150). For stem-like ($CD8^+$ $PD1^+$ $LAG3^-$ $TCF1^+$ $GranzymeB^-$), better effector ($CD8^+$ $PD1^+$ $LAG3^-$, $TCF1^-$, $GranzymeB^+$) and exhausted ($CD8^+$ $PD1^+$ $LAG3^+$ $TCF1^-$ $GranzymeB^-$) T cells: Live/Dead Fixable Near-IR Dead Cell Stain Kit, CD8 BV510, PD1 BV421 (clone 29F.1A12, BioLegend; cat. 135217); LAG3 PE-Cy7 (clone c9b7w, BioLegend; cat. 125226). For intracellular staining, cells were fixed with Cytofix/Cytoperm Fixation/Permeabilization Kit (BD; cat. 554714) and then stained for Granzyme B FITC (clone GB11, BioLegend; cat. 515403) and TCF1 APC (clone C63D9, Cell Signaling; cat. 37636S). For regulatory T cells (Tregs): Live/Dead Fixable Near-IR Dead Cell Stain Kit, CD3 FITC (clone 145–2C1, BD; cat. 553062); CD8 BV510, CD4 PE-Cy7. For intracellular staining, forkhead box P3 (Foxp3)/Transcription Factor Staining Buffer Set (eBioscience, cat. 00-5523-00) was used and then cells were stained with Foxp3 APC (clone FJK-16s, eBioscience; cat. 00-5523-00).

FACSCanto II was used for data acquisition and FlowJo (V.10) was used for the analysis.

Statistical analysis

The data are presented as means±SEM. For statistical analysis, significance was tested using the Student's t-test, one-way analysis of variance (ANOVA), and two-way ANOVA with Fisher's least significant Difference (LSD) or Tukey's post hoc tests. A minimum value of $p<0.05$ was considered statistically significant. Statistical analysis was performed using GraphPad Prism V.10.

RESULTS

Selection of a murine model for testing neoadjuvant/adjuvant vaccination effectiveness

To identify the most suitable tumor model for evaluating the therapeutic efficacy of neoadjuvant and adjuvant immunotherapies, including nAg-targeted vaccines and CPIs, we compared the relapse rate after surgical tumor resection in different tumor models: colon carcinoma (CT26 and MC38), mammary tumor (4T1) and melanoma (B16F10) (scheme in figure 1A). No or low relapse rate postsurgery was observed in the CT26 (figure 1B), 4T1 (figure 1C) and MC38 (figure 1D) models. In contrast, a high rate of tumor recurrence (75%) was observed in the B16F10 melanoma model (figure 1E), making it the most appropriate model to use for investigating the effectiveness of neoadjuvant and adjuvant treatments in all the subsequent experiments.

GAd vaccine encoding B16F10 neoantigens induces potent neoantigen-specific T-cell response

A B16F10 nAg-based cancer vaccine was generated. S.c. B16F10 tumors were excised from mice and processed for whole exome sequencing to identify the nAgs to target in the vaccine. 62 candidate nAgs were selected using the

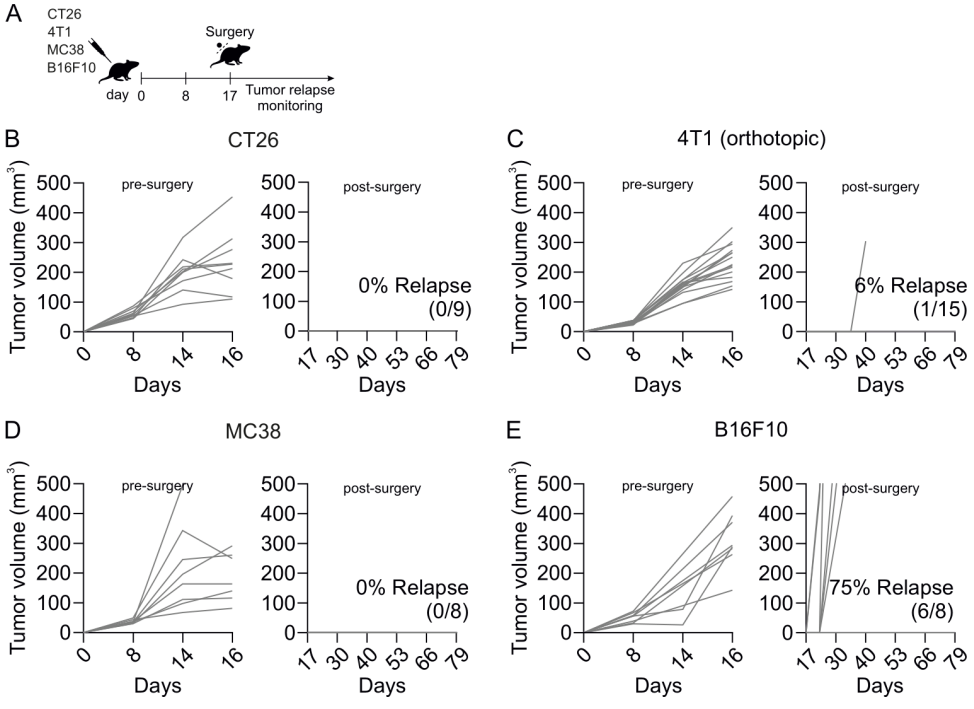

Figure 1 Relapse rate postsurgery across different tumor models. (A) Schematic representation of the experimental setting. Tumor growth of (B) CT26, (C) 4T1, (D) MC38 and (E) B16F10 was monitored before surgery (day 17) and tumor relapse was monitored after surgery. Lines in the graphs represent each individual tumor. Percentages on the graphs indicate the rate of relapse. The number of experimental mice (n≥8) is indicated in each graph.

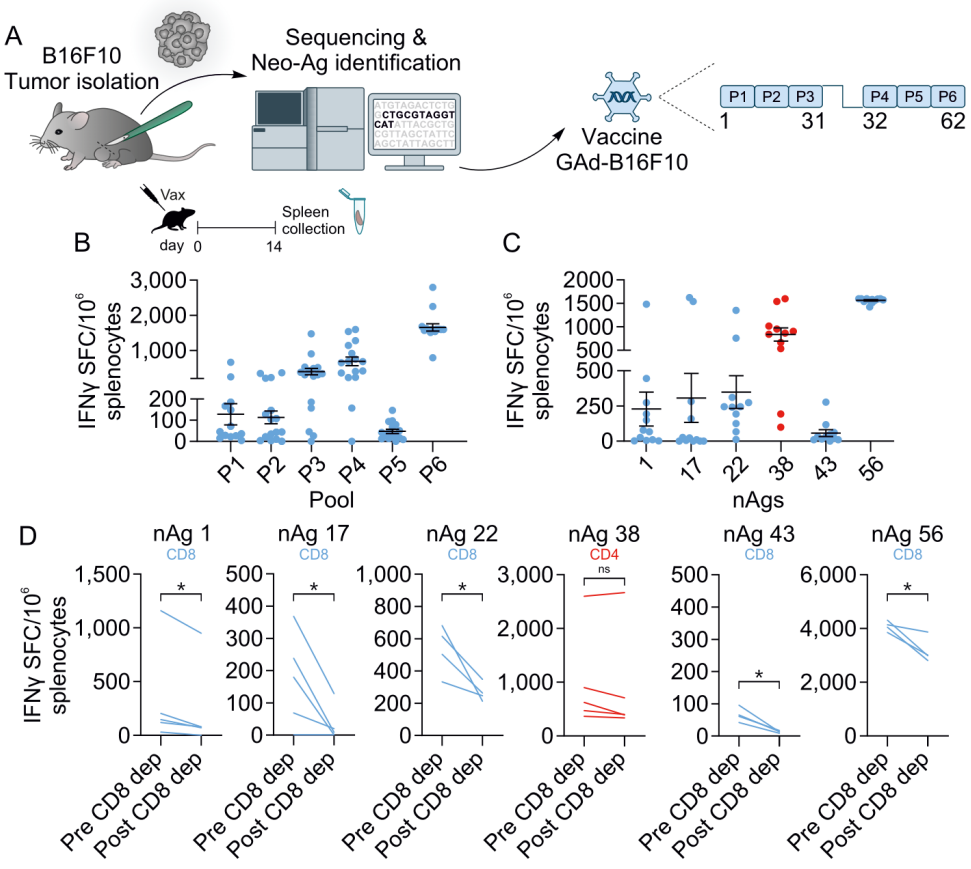

Figure 2 In vivo immunogenicity of GAd encoding B16F10 nAgs. (A) Schematic representation of 62 B16F10 nAgs selection and GAd-B16F10 vaccine generation. (B–D) In vivo immunogenicity of GAd-B16F10 vaccine by IFNγ ELISpot on splenocytes of naive C57BL/6 mice (n ≥ 10). Results are shown as IFNγ SFC normalized per million of splenocytes. (B) Responses against six pools (P1–P6) covering all 62 nAgs or (C) individual immunogenic nAgs identified after deconvolution are shown. Blue and red dots indicate nAgs inducing $CD8^+$ and $CD4^+$ T cell responses, respectively. (D) IFNγ ELISpot performed on $CD8^+$ T cell-depleted splenocytes and responses against the indicated nAg are represented, pre and post depletion. A paired t-test was performed to obtain p values. *p<0.05. GAd, Great-Ape Adenoviral; IFNγ, interferon-gamma; nAgs, neoantigens; SFC, spot forming colonies.

VENUS algorithm, and were encoded into a GAd vector (GAd-B16F10), as previously described[6 20] (figure 2A and online supplemental table 1). Then, the immunogenicity of the GAd-B16F10 vaccine was assessed on freshly isolated splenocytes from immunized mice using ex vivo IFNγ ELISpot assay. Cells were isolated and stimulated with six peptide pools (P1-P6), each containing 10 25-mer peptides, with the exception of P6, which included 12 25-mer peptides. nAg-specific T cell responses were reported for each pool, with the highest reactivity observed against P3, P4, and P6 (figure 2B). Full deconvolution to map the individual reactive peptides within each pool revealed six highly immunogenic nAgs, with epitope 56 being the most immunogenic (figure 2C). In addition, the GAd-B16F10 vaccine included nAgs able to induce $CD8^+$ (blue dots) and $CD4^+$ (red dots) T cells, as assessed by IFNγ ELISpot post $CD8^+$ T cell depletion (figure 2D).

GAd-B16F10 vaccine is highly effective in the neoadjuvant setting

In a setting of therapeutic treatment of large established B16F10 tumors, the antitumor efficacy of GAd-B16F10 vaccine was low, eradicating tumors in only 20% of mice when combined with anti-PD1 (blue curves), compared with 0% with anti-PD1 alone (pink curves) (figure 3A). This result confirms that the B16F10 model is highly resistant to immunotherapy.[21] The efficacy of the GAd-B16F10 vaccine was therefore evaluated in a different therapeutic approach, exploring vaccine activity in the neoadjuvant and adjuvant settings in the context of surgical tumor resection. Administration schedules are shown in figure 3B. Surgery was performed on tumors with an average volume of 400–600 mm^3 (online supplemental figure 1A). In the absence of treatment, a high tumor relapse rate of 75% was observed after surgery (figure 3C, black bar). Neoadjuvant vaccination alone reduced the relapse rate to 30% and, when combined with anti-PD1, to 10% (figure 3C, light and dark blue bar, respectively). In contrast, adjuvant vaccination alone resulted in a 65% relapse rate which was reduced to 35% when vaccination was combined with anti-PD1 (figure 3C, light and dark green bar, respectively). Mice receiving anti-PD1 before or after surgery relapsed at 40% and 60% rate, respectively (figure 3C, light and dark pink bar, respectively).

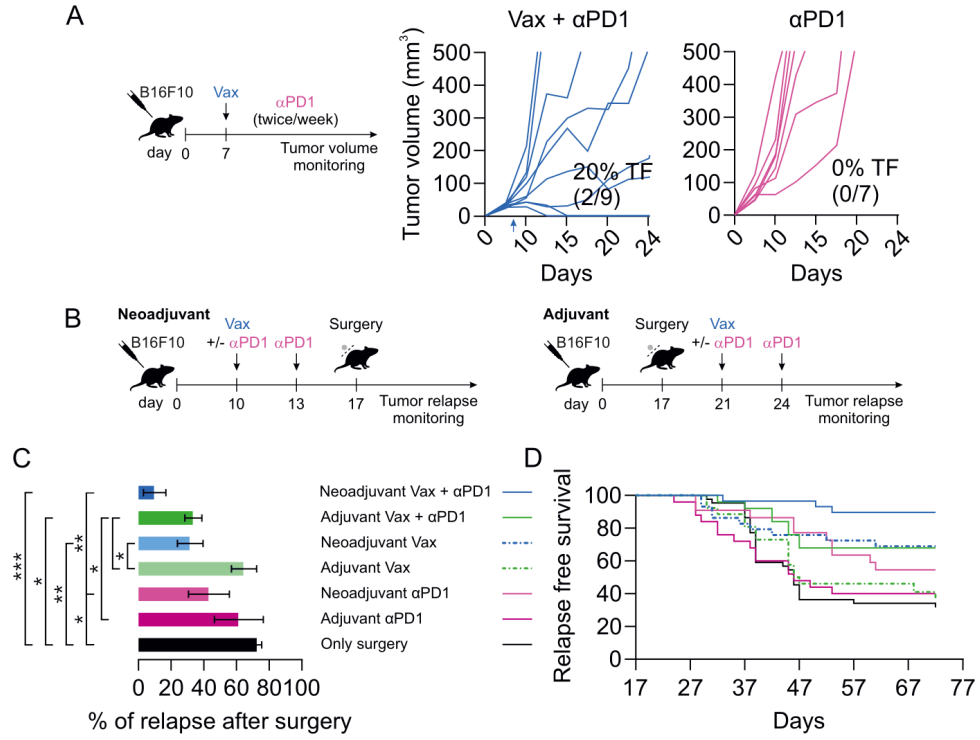

Figure 3 GAd-B16F10 vaccine is ineffective in advanced tumor setting but protects from tumor relapse in the neoadjuvant setting. (A) Schematic representation of advanced therapeutic setting and tumor growth monitoring. C57BL/6 mice (n≥7) were inoculated with B16F10 cells. After 7 days mice were immunized with GAd-B16F10 vaccine in combination with anti-PD1. Mice treated with anti-PD1 alone were used as control. Lines in the graphs represent each individual tumor. Percentages on the graphs indicate the rate of TF mice and the number of experimental mice is indicated in each graph. (B) Schematic representation of neoadjuvant and adjuvant settings. C57BL/6 mice (n≥13) were injected with B16F10 cells (day 0). In the neoadjuvant setting, mice were immunized with GAd-B16F10 vaccine (day 10) in combination or not with two injections of anti-PD1 (day 10 and day 13) or received only anti-PD1 (day 10 and day 13). All mice underwent surgery for tumor removal on day 17. In the adjuvant setting, after 17 days from tumor inoculum, mice underwent tumor surgery and after 4 days (day 21) were immunized with GAd-B16F10 vaccine in combination or not with two injections of anti-PD1 (day 21 and day 24) or received anti-PD1 alone (day 21 and day 24). As a control group, mice were subjected only to surgery, without treatment. (C) Relapse rate after surgery. Each bar represents the percentage of tumor relapse per experimental group. (D) Relapse-free survival after surgery. Each curve indicates the percentage of survival of relapse-free mice per experimental group. Data are presented as mean±SEM. Ordinary one-way ANOVA with Fisher's Least Significant Difference (LSD) test was performed to obtain p values. *p<0.05, **p<0.005, ***p<0.001. ANOVA, analysis of variance; GAd, Great-Ape Adenoviral; LSD, least significant difference; PD1, programmed cell death protein 1; TF, tumor free.

Results were confirmed by examining the relapse-free survival (figure 3D). These findings suggest that the GAd-B16F10 vaccine is more effective in protecting from tumor relapse in the neoadjuvant setting compared with the adjuvant setting, even when used as monotherapy, showing the best therapeutic effect when combined with anti-PD1. In contrast, the GAd-B16F10 vaccine was effective in the adjuvant setting only in combination with CPI. The relapse rate was independent of tumor volume at the time of surgery (online supplemental figure 1B).

Neoadjuvant GAd-B16F10 efficacy is CD8 dependent and induces changes in intratumoral CD8$^+$ phenotype

We next focused on the most effective treatment of neoadjuvant vaccine plus anti-PD1. To assess whether the efficacy of GAd-B16F10 vaccine in combination with anti-PD1 in neoadjuvant setting was T-cell dependent, CD8$^+$ and CD4$^+$ T cells were depleted with anti-CD8 or anti-CD4 antibodies respectively, as shown in the scheme depicted in figure 4A. The selective depletion of CD8$^+$ T cells completely abolished the vaccine's effectiveness, resulting in 100% tumor relapse after surgery (figure 4B). In contrast, depleting CD4$^+$ T cells had no impact (figure 4C). The undepleted T cell control group showed no relapse after surgery (figure 4D). To get insights on the different efficacy of the tested neoadjuvant therapies, we analyzed the tumor immune infiltrate at the time of surgery (figure 4E). To explore the generation of vaccine-induced T cells, we selected nAg 1 (based on dextramer availability) and nAg 56 (as the most immunogenic). These antigen-specific T cells were detectable in the tumors at the time of surgery (figure 4F) in vaccinated mice, and showed almost entirely, an EM phenotype (CD44$^+$CD62L$^-$) (figure 4I). After 4 days from surgery, an increase in vaccine-induced antigen-specific T cells was observed in tdLNs, indicating that they persist after tumor removal (online supplemental figure 2). Regarding the

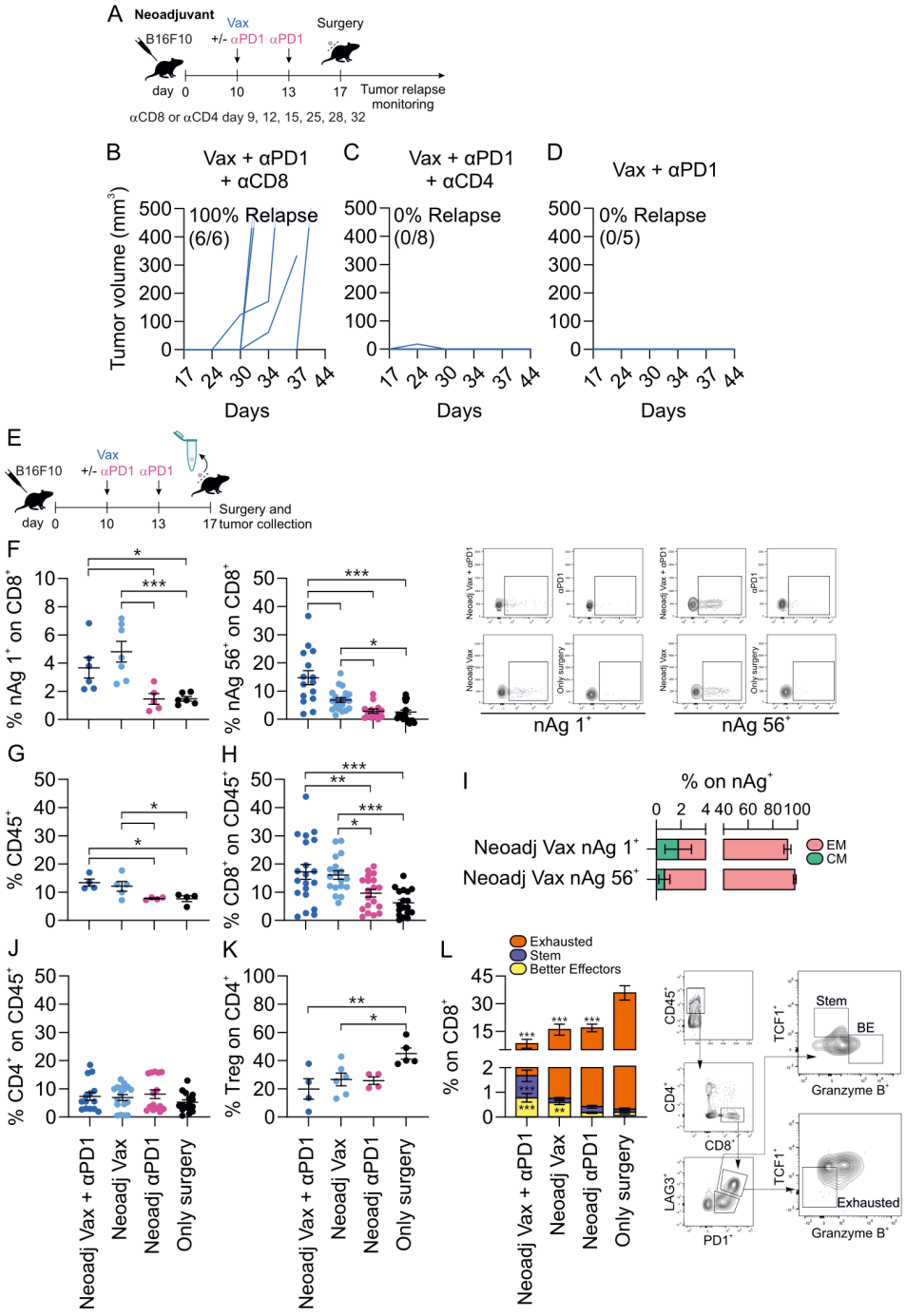

Figure 4 Neoadjuvant GAd-B16F10 efficacy is CD8-dependent, expands intratumoral antigen-specific CD8$^+$ T cells and induces phenotypical changes in CD8$^+$ T cells. (A) Schematic representation of in vivo CD8$^+$ and CD4$^+$ T-cell depletion. C57BL/6 mice (n≥5) were inoculated with B16F10 cells and after 10 days, mice were vaccinated with GAd-B16F10 in combination with anti-PD1 (day 10 and day 13) and (B) anti-CD8 or (C) anti-CD4 (day 9, 12, 15, 25, 28, 32) or (D) without depleting antibodies. At day 17, mice underwent surgery for tumor excision and were monitored for tumor relapse over time. Lines in the graphs represent each individual tumor. Percentages on the graphs indicate the rate of relapse and the number of experimental mice is indicated in each graph. (E) Schematic representation of neoadjuvant setting and tumor collection for FACS analysis. (F) Tumors (n≥4) collected at day of surgery (day 17) were analyzed for vaccine-induced antigen-specific T cells, nAg 1 and nAg 56 with their representative plots; (G) for intratumoral CD45$^+$ immune cells and (H) CD8$^+$ T cells. (I) Focus on antigen-specific T cell memory phenotypes (EM: CD44$^+$ CD62L$^-$ and CM: CD44$^+$ CD62L$^+$). (J) Tumors of (F) were analyzed for CD4$^+$ T cells and (K) Tregs (CD4$^+$ FoxP3$^+$) cells. (L) Focus on CD8$^+$ phenotypes: stem-like (LAG3$^-$ PD1$^+$ Granzyme B$^-$ TCF1$^+$), better effector (LAG3$^-$ PD1$^+$ Granzyme B$^+$ TCF1$^-$) and exhausted (LAG3$^+$ PD1$^+$ Granzyme B$^-$ TCF1$^-$) CD8$^+$ T cells, with the relative gating strategy; Data are presented as mean±SEM. Ordinary one-way ANOVA with Fisher's LSD test was performed to obtain P values. *p<0.05, **p<0.005, ***p<0.001. ANOVA, analysis of variance; CM, central memory; EM, effector memory; FACS, fluorescence-activated cell sorting;GAd, Great-Ape Adenoviral; LSD, least significant difference; nAg, neoantigen; PD1, programmed cell death protein 1; Treg, regulatory T cell.

impact of neoadjuvant treatments on the bulk tumor lymphocytic infiltrate, we observed a significant increase of intratumoral CD45$^+$ immune cells (figure 4G) and CD8$^+$ T cells (figure 4H) in mice treated with the vaccine, either alone or in combination with anti-PD1, compared with mice treated with anti-PD1 alone or the untreated controls.

In untreated tumors, there was an enrichment of exhausted CD8$^+$ T cells. On administration of neoadjuvant vaccine or anti-PD1, a significant reduction in the frequency of these cells was observed. This decrease was more pronounced when both therapies were combined (figure 4L, orange bars). Additionally, tumors from neoadjuvant-vaccinated mice exhibited higher levels of better effector CD8$^+$ T cells, regardless of whether they received the anti-PD1 combination (figure 4L, yellow bars), whereas an increase in stem-like CD8$^+$ T cells was observed only in mice receiving the combination of vaccine and anti-PD1 (figure 4L, purple bar). The frequency of CD4$^+$ T cells remained similar across all groups (figure 4J). However, intratumoral Tregs were enriched in untreated mice with a significant reduction following vaccine administration (figure 4K).

GAd20-B16F10 vaccine protects from relapse to a second rechallenge and induces long-lasting memory

Tumor-free mice with no relapse after treatment with neoadjuvant GAd-B16F10 vaccine alone or in combination with anti-PD1, or anti-PD1 alone, were subjected to a second challenge with B16F10 cells (figure 5A). Mice that had received neoadjuvant vaccination, either alone or with anti-PD1, were effectively protected with only approximately 10% of mice experiencing relapse, demonstrating durable vaccine-induced immunity (figure 5B, light and dark blue bars). In contrast, 80% of mice that had received neoadjuvant anti-PD1 relapsed after the second challenge (figure 5B, pink bar). Neoadjuvant vaccination, either alone or in combination with anti-PD1 also demonstrated a significant control on distant metastases following a third tumor challenge by intravenous injection of B16F10 cells. After 20 days, lungs were collected and analyzed for metastatic burden by counting nodules. Mice receiving neoadjuvant treatment developed a significantly lower number of metastases compared with untreated controls (figure 5C).

To investigate the mechanism behind the protection from second tumor recurrence, we compared the circulating T cells in mice treated with neoadjuvant-vaccine plus or minus anti-PD1 and neoadjuvant anti-PD1 alone, at different days after surgery and rechallenge (figure 5A). Although overall CD8$^+$ T cell levels remained comparable between groups over time (figure 5D), neoadjuvant-vaccinated mice consistently showed higher EM CD8$^+$ T cell levels, regardless of anti-PD1 cotreatment, when compared with anti-PD1 alone. CM CD8$^+$ T cell levels were similar across groups (figure 5E). The analysis of circulating antigen-specific T cells also showed higher levels of nAg 56$^+$ T cells in vaccinated mice compared with anti-PD1 monotherapy (figure 5F), with a phenotype of EM (figure 5G). In anti-PD1 treated mice, nAg 56$^+$ T cells were below the detection level, indicating that these cells were generated and expanded by the vaccination (figure 5F).

Similar findings were observed at later time points (online supplemental figure 3A-D). The levels of nAg 1$^+$ T cells were also investigated and found similar between groups, suggesting that these cells are likely to be pre-existing and tumor-induced (online supplemental figure 3E,F).

Neoadjuvant GAd-B16F10 vaccine alters CD8$^+$ T cell phenotypes in tumor-draining lymph nodes, promoting effector functions

To investigate the differences between neoadjuvant and adjuvant vaccination, we analyzed the CD8$^+$ T cells in the tdLNs of treated mice (figure 6A and online supplemental figure 4A). Three weeks after treatment, brachial and axillary lymph nodes were collected for the analysis (figure 6A and online supplemental figure 4A). TdLNs from neoadjuvant-vaccinated mice showed a significantly higher frequency of CD8$^+$ T cells compared with adjuvant vaccinated mice (figure 6B), although no differences were observed when compared with anti-PD1 treated mice, either in neoadjuvant or adjuvant setting (online supplemental figure 4B). Further analysis of CD8$^+$ T cell phenotypes revealed that neoadjuvant vaccination, compared with adjuvant treatment, significantly increased the proportions of stem-like (PD1$^+$ LAG3$^-$ TCF1$^+$ GranzymeB$^-$) (figure 6C) and better effector (PD1$^+$ LAG3$^-$ TCF1$^-$ GranzymeB$^+$) (figure 6D) CD8$^+$ T cells, which were not observed in anti-PD1-treated mice (online supplemental figure 4C,D), while both neoadjuvant vaccination and anti-PD1 treatment led to a reduction in exhausted (PD1$^+$ LAG3$^+$ TCF1$^-$ GranzymeB$^-$) CD8$^+$ T cells compared with their respective adjuvant controls (figure 6E, online supplemental figure 4E). In the spleen, vaccination induced comparable immune responses in both neoadjuvant and adjuvant settings (online supplemental figure 5A,B). Both treatment groups similarly expanded circulating CD8$^+$ T cells (online supplemental figure 5C,D), EM CD8$^+$ T cells (online supplemental figure 5E), and generated Ag-specific T cells with an EM phenotype (online supplemental figure 5F,G).

DISCUSSION

nAg-based vaccines are a potent means of generating tumor-specific T cell responses. Recent clinical studies exploring the efficacy of personalized cancer vaccines in the adjuvant setting have shown promising clinical responses with a significant improvement in patients' recurrence-free survival and a positive correlation between vaccine-expanded T cells and clinical outcome in several tumor indications, including pancreatic and renal cancers and melanoma.[9 10 12] To date, the potential advantage of neoadjuvant over adjuvant nAg vaccination

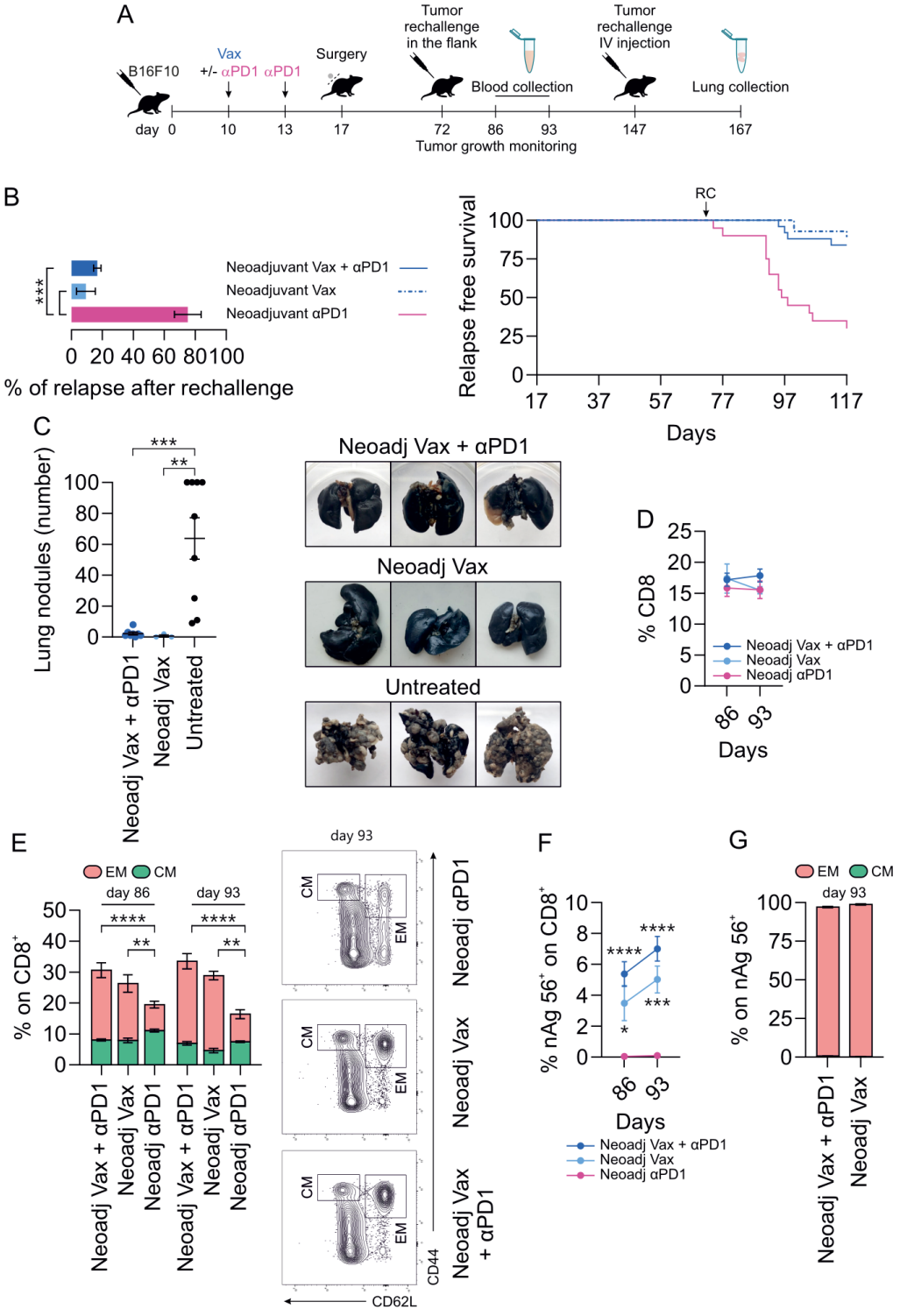

Figure 5 Neoadjuvant GAd-B16F10 induces long-term memory and provides protection against tumor rechallenge. (A) Schematic representation of tumor rechallenge in relapse-free survival mice from neoadjuvant treated mice (n≥13). (B) Bars and curves represent the percentage of relapsed mice and relapse-free survival rates after tumor rechallenge (day 72), respectively. (C) Relapse-free survival mice from GAd-B16F10+anti-PD1 group (n=8), GAd-B16F10 alone (n=3) and untreated mice (n=9) were injected i.v. with B16F10 cells at day 147 and after 20 days, lungs were collected for metastases analysis. The graph indicates the number of lung nodules. Representative lung pictures are shown. (D–G) Blood collection was performed at day 86 and 93 and analyzed by flow cytometry. Graphs indicate (D) the percentage of $CD8^+$ T cells, (E) the memory phenotype of $CD8^+$ T cells (EM: $CD8^+$ $CD44^+$ $CD62L^-$, CM: $CD8^+$ $CD44^+$ $CD62L^+$) and representative FACS plots, (F) the percentage of nAg 56^+ cells, (G) the memory phenotype of nAg 56^+-specific T cells. Data are presented as mean±SEM. Ordinary one-way ANOVA with Fisher's LSD test was performed to obtain p values. *p<0.05, **p<0.005, ***p<0.001, ****p<0.0001. ANOVA, analysis of variance; CM, central memory; EM, effector memory; FACS, fluorescence-activated cell sorting; GAd, Great-Ape Adenoviral; IV, intravenous; LSD, Least Significant Difference; nAg, neoantigen; PD1, programmed cell death protein 1; RC, rechallenge.

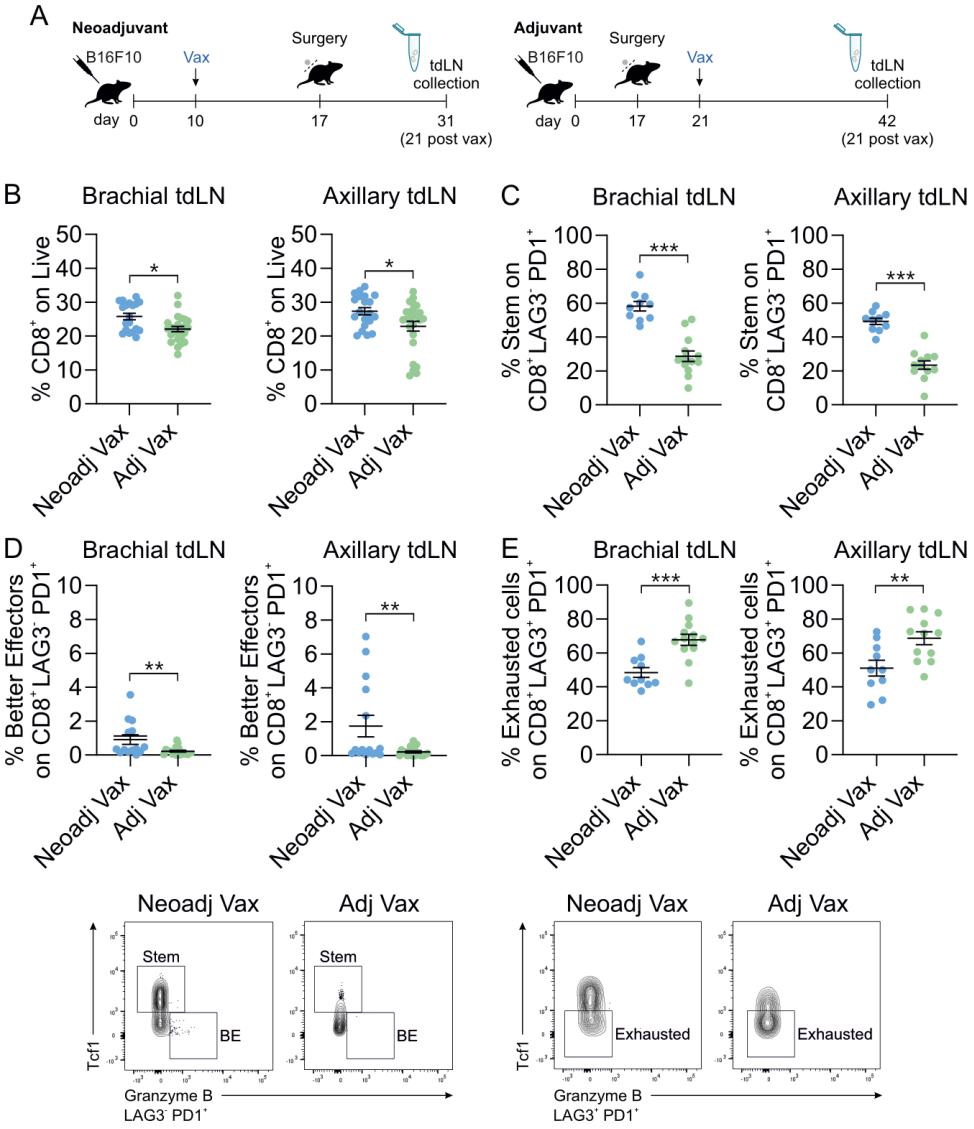

Figure 6 Neoadjuvant GAd-B16F10 vaccination induces phenotypical changes in CD8$^+$ T cell in tdLNs, compared with adjuvant setting. (A) Schematic representation of tdLNs collection for flow cytometry analysis in neoadjuvant and adjuvant setting. (B) Percentage of CD8$^+$, (C) stem-like (CD8$^+$ LAG3$^-$ PD1$^+$ Granzyme B$^-$ TCF1$^+$), (D) better effectors (CD8$^+$ LAG3$^-$ PD1$^+$ Granzyme B$^+$ TCF1$^-$), (E) exhausted (CD8$^+$ LAG3$^+$ PD1$^+$ Granzyme B$^-$ TCF1$^-$) in brachial and axillary lymph nodes and representative FACS plots. Data are presented as mean±SEM. Ordinary one-way ANOVA with Fisher's LSD test was performed to obtain p values. *p<0.05, **p<0.005, ***p<0.001. ANOVA, analysis of variance; FACS, fluorescence-activated cell sorting;GAd, Great-Ape Adenoviral; LSD, least significant difference; PD1, programmed cell death protein 1; tdLN, tumor-draining lymph node.

has yet to be evaluated. In this study, we assessed the impact of adjuvant versus neoadjuvant nAg-based vaccination as monotherapy and in combination with anti-PD1 in the CPI-resistant preclinical model of B16F10. Our data demonstrated that vaccination was ineffective when given after tumor resection and required the combination with anti-PD1 to achieve protection from relapse. In contrast, monotherapy vaccination in the neoadjuvant setting provided superior effectiveness compared with the adjuvant vaccination, improving the recurrence-free survival and reaching the highest activity when combined with anti-PD1. Our findings support the hypothesis that immunization prior to tumor resection can enhance immune priming and generate a more effective antitumor response. The improved efficacy of neoadjuvant vaccination compared with adjuvant administration is likely due to the presence of the tumor at the time of vaccination, allowing for more robust antigen presentation and enhanced systemic T cell immunity. For an immune response to be effective, tumor cells, antigen-presenting cells, and T cells need to interact closely. These interactions are more likely when the tumor is still in place, which may explain why CPI and vaccines work better before surgery. In line with this hypothesis, several studies have shown that T cell expansion is stronger when CPI is given before surgery rather than after.[22] In addition to the relative timing of immunotherapy to surgical tumor resection, another aspect to consider is the timing

relative to the administration of CPI and vaccination. In our study, anti-PD1 was administered concurrently and very shortly after vaccination, resulting in a strong synergism. This is supported by recent findings demonstrating that there is a timing-dependent factor relative to the combination of vaccination and anti-PD1, supporting that anti-PD1 is more effective when employed at the time of $CD8^+$ T cell activation.[23] The superiority of neoadjuvant versus adjuvant immunotherapy has been demonstrated in preclinical models of breast cancer, where the administration of CPI before surgery was associated with higher and sustained peripheral tumor-specific immune responses.[14] In the context of cancer vaccine, consistent with our data, Grinshtein *et al* showed that neoadjuvant vaccination against human melanoma antigen Tyrosinase-related protein 2, was superior to adjuvant vaccination in a preclinical model.[13] A key distinction with our study is the choice of the tumor antigen, in our case nAgs versus tumor-associated antigens, the latter being subject to central and peripheral immune tolerance, limiting the magnitude and durability of the T cell responses they can elicit and, as a consequence, expected to be less effective in clinical trials.[24]

The therapeutic response of neoadjuvant vaccine plus anti-PD1 was completely lost when $CD8^+$ T cells were depleted, indicating that these cells are the drivers of the antitumor activity. Anti-PD1 therapy alone also worked well in the neoadjuvant setting, however, combining it with the vaccine produced the most effective outcome, suggesting that anti-PD1 helps vaccine-primed T cells stay active and avoid exhaustion. Indeed, the addition of nAg vaccination to anti-PD1 further amplified antitumor immunity. This likely reflects the vaccine's ability to broaden and deepen the T cell response repertoire. At the time of surgery, neoadjuvant vaccinated mice presented higher levels of intratumoral $CD8^+$ and vaccine-induced antigen-specific T cells, compared with neoadjuvant anti-PD1 treated and untreated mice. We also observed enrichment of intratumoral stem-like and better effector T cells and low levels of exhausted T cells. These findings are in line with our previous preclinical and clinical studies demonstrating that GAd vaccines targeting tumor nAgs in combination with anti-PD1 are able to broaden the antigenic breadth and clonal diversity of $CD8^+$ T cells, resulting in tumor infiltration of vaccine-induced nAg-specific T cells.[25 26] The therapeutic effect of GAd vaccines depends on both the magnitude and the quality of vaccine-induced $CD8^+$ T cells. In mice, a combination of GAd and anti-PD1 has been shown to promote the generation of stem-like T cell reservoir for a more effective antitumor activity.[6 26]

Interestingly, tumor rechallenge experiments revealed a striking difference in long-term protection between neoadjuvant vaccination (alone and combined with anti-PD1) and neoadjuvant anti-PD1 alone, the latter showing a significantly higher relapse rate, with only 20% remaining tumor-free.

In line with this observation, neoadjuvant vaccination resulted in a higher proportion of circulating antigen-specific T cells persisting in the blood of mice remaining tumor-free after rechallenge (126 days after surgery) and a higher percentage of circulating $CD8^+$ T cells with $CD44^+$ $CD62L^-$ EM phenotype compared with anti-PD1. This suggests that neoadjuvant vaccination but not neoadjuvant anti-PD1 alone was able to generate long-lasting immune EM. As such, these findings underscore the superior durability of vaccine-induced immunity and suggest that while checkpoint blockade can reinvigorate pre-existing T cells, it may not be sufficient to generate long-lasting immune memory on its own. In contrast, the vaccine appears to prime a broader, more sustained $CD8^+$ T cell response capable of recognizing and eliminating recurrent tumor cells.

To address the mechanism behind the different therapeutic outcomes observed in neoadjuvant and adjuvant vaccination, we focused our attention on lymphoid organs and peripheral blood, as direct evaluation of the tumor microenvironment is not feasible in the adjuvant setting following tumor removal. A difference between neoadjuvant and adjuvant vaccination was observed in the tdLNs, which serve as critical sites for T cell priming and differentiation. In murine models, removal of tdLNs has been associated with reduced survival postsurgery, suggesting that they play a key role in controlling tumor relapse. In neoadjuvant-treated mice, tdLNs showed a significantly higher frequency of $CD8^+$ T cells, particularly those enriched in stem-like and superior effector subsets. These populations are associated with enhanced proliferative capacity, responsiveness to checkpoint blockade, and the ability to sustain long-term antitumor responses. Stem-like $CD8^+$ T cells act as reservoirs for ongoing immune surveillance and memory formation, while better effector T cells exhibit strong cytotoxic function and tumor-homing potential. Concurrently, exhausted T cells were reduced in the neoadjuvant setting. In the spleen, similar levels of vaccine-induced antigen-specific immune responses, and circulating antigen-specific T cells were detected in both neoadjuvant and adjuvant settings. These differences underline the immunological advantage of neoadjuvant vaccination: by presenting tumor antigens in the context of an intact tumor microenvironment, the immune system is exposed to both antigen and inflammatory cues that may drive more robust and functional T cell responses.

Despite the strong preclinical rationale, no clinical trials have yet investigated personalized cancer vaccines in the neoadjuvant setting, largely due to the complexities of timely manufacturing. Personalized cancer vaccines must be produced within a strict timeline to ensure they are available before tumor resection, allowing adequate time for T cell activation and tumor elimination. Adopting neoadjuvant personalized cancer vaccines in clinical practice will necessitate significant adjustments in treatment protocols. However, with ongoing advancements in vaccine manufacturing technologies and mounting evidence that neoadjuvant immunotherapies offer superior benefits to patients, this approach might become

feasible and effective, offering a new frontier in cancer immunotherapy.

Acknowledgements We acknowledge the animal facility of Plaisant in Castel Romano (Rome) for maintenance and care of the mice used in this study. We would like to thank Domenico Salvatori for his support with tumor calibrations for in vivo studies.

Contributors ES is the guarantor of the work. Designing research studies: AMD, ES; developing methods: LS, LN, GL, GC, FT, GR, TB, EM, IG, LA; conducting experiments and acquiring data: LS, LN, GL, GC, FT, GR, TB, EM, IG, LA; data analysis: LS, LN; preparing figures: AMD, ES, LS, LN; funding acquisition: ES; project administration: AMD, ES; supervision: AMD, ES; writing—original draft: AMD, LS, LN; writing—review and editing: ES. LS and LN contributed equally to this work.

Funding The authors have not declared a specific grant for this research from any funding agency in the public, commercial or not-for-profit sectors.

Competing interests ES is the founder of Nouscom. AMD, LS, LN, GC, FT, GR, TB, EM, IG, LA are employees of Nouscom.

Patient consent for publication Not applicable.

Ethics approval Not applicable.

Provenance and peer review Not commissioned; externally peer reviewed.

Data availability statement All data relevant to the study are included in the article or uploaded as supplementary information.

ORCID iDs
Laura Seclì https://orcid.org/0000-0001-7129-3355
Linda Nocchi https://orcid.org/0000-0002-2113-9031
Fulvia Troise https://orcid.org/0000-0002-4815-1495
Teresa Busiello https://orcid.org/0009-0003-6258-1568
Elisa Scarselli https://orcid.org/0000-0002-5393-6713
Anna Morena D'Alise https://orcid.org/0000-0002-0763-6269

REFERENCES

1 Patel SP, Othus M, Chen Y, *et al*. Neoadjuvant-Adjuvant or Adjuvant-Only Pembrolizumab in Advanced Melanoma. *N Engl J Med* 2023;388:813–23.
2 Eggermont AMM, Chiarion-Sileni V, Grob J-J, *et al*. Prolonged Survival in Stage III Melanoma with Ipilimumab Adjuvant Therapy. *N Engl J Med* 2016;375:1845–55.
3 Eggermont AMM, Kicinski M, Blank CU, *et al*. Five-Year Analysis of Adjuvant Pembrolizumab or Placebo in Stage III Melanoma. *NEJM Evid* 2022;1:EVIDoa2200214.
4 Weber J, Mandala M, Del Vecchio M, *et al*. Adjuvant Nivolumab versus Ipilimumab in Resected Stage III or IV Melanoma. *N Engl J Med* 2017;377:1824–35.
5 Grinshtein N, Ventresca M, Margl R, *et al*. High-dose chemotherapy augments the efficacy of recombinant adenovirus vaccines and improves the therapeutic outcome. *Cancer Gene Ther* 2009;16:338–50.
6 D'Alise AM, Leoni G, Cotugno G, *et al*. Adenoviral vaccine targeting multiple neoantigens as strategy to eradicate large tumors combined with checkpoint blockade. *Nat Commun* 2019;10:2688.
7 Garzia I, Nocchi L, Avalle L, *et al*. Tumor Burden Dictates the Neoantigen Features Required to Generate an Effective Cancer Vaccine. *Cancer Immunol Res* 2024;12:440–52.
8 McAuliffe J, Chan HF, Noblecourt L, *et al*. Heterologous prime-boost vaccination targeting MAGE-type antigens promotes tumor T-cell infiltration and improves checkpoint blockade therapy. *J Immunother Cancer* 2021;9:e003218.
9 Weber JS, Carlino MS, Khattak A, *et al*. Individualised neoantigen therapy mRNA-4157 (V940) plus pembrolizumab versus pembrolizumab monotherapy in resected melanoma (KEYNOTE-942): a randomised, phase 2b study. *Lancet* 2024;403:632–44.
10 Rojas LA, Sethna Z, Soares KC, *et al*. Personalized RNA neoantigen vaccines stimulate T cells in pancreatic cancer. *Nature New Biol* 2023;618:144–50.
11 Sethna Z, Guasp P, Reiche C, *et al*. RNA neoantigen vaccines prime long-lived CD8$^+$ T cells in pancreatic cancer. *Nature New Biol* 2025;639:1042–51.
12 Braun DA, Moranzoni G, Chea V, *et al*. A neoantigen vaccine generates antitumour immunity in renal cell carcinoma. *Nature New Biol* 2025;639:474–82.
13 Grinshtein N, Bridle B, Wan Y, *et al*. Neoadjuvant vaccination provides superior protection against tumor relapse following surgery compared with adjuvant vaccination. *Cancer Res* 2009;69:3979–85.
14 Liu J, Blake SJ, Yong MCR, *et al*. Improved Efficacy of Neoadjuvant Compared to Adjuvant Immunotherapy to Eradicate Metastatic Disease. *Cancer Discov* 2016;6:1382–99.
15 Liu J, O'Donnell JS, Yan J, *et al*. Timing of neoadjuvant immunotherapy in relation to surgery is crucial for outcome. *Oncoimmunology* 2019;8:e1581530.
16 Blank CU, Rozeman EA, Fanchi LF, *et al*. Neoadjuvant versus adjuvant ipilimumab plus nivolumab in macroscopic stage III melanoma. *Nat Med* 2018;24:1655–61.
17 Cloughesy TF, Mochizuki AY, Orpilla JR, *et al*. Neoadjuvant anti-PD-1 immunotherapy promotes a survival benefit with intratumoral and systemic immune responses in recurrent glioblastoma. *Nat Med* 2019;25:477–86.
18 Blank CU, Lucas MW, Scolyer RA, *et al*. Neoadjuvant Nivolumab and Ipilimumab in Resectable Stage III Melanoma. *N Engl J Med* 2024;391:1696–708.
19 O'Donnell JS, Hoefsmit EP, Smyth MJ, *et al*. The Promise of Neoadjuvant Immunotherapy and Surgery for Cancer Treatment. *Clin Cancer Res* 2019;25:5743–51.
20 Leoni G, D'Alise AM, Tucci FG, *et al*. VENUS, a Novel Selection Approach to Improve the Accuracy of Neoantigens' Prediction. *Vaccines (Basel)* 2021;9:880.
21 Jaiswal AR, Liu AJ, Pudakalakatti S, *et al*. Melanoma Evolves Complete Immunotherapy Resistance through the Acquisition of a Hypermetabolic Phenotype. *Cancer Immunol Res* 2020;8:1365–80.
22 Llovet JM, Pinyol R, Yarchoan M, *et al*. Adjuvant and neoadjuvant immunotherapies in hepatocellular carcinoma. *Nat Rev Clin Oncol* 2024;21:294–311.
23 Moseman JE, Rastogi I, Jeon D, *et al*. PD-1 blockade employed at the time CD8+ T cells are activated enhances their antitumor efficacy. *J Immunother Cancer* 2025;13:e011145.
24 Nüssing S, Trapani JA, Parish IA. Revisiting T Cell Tolerance as a Checkpoint Target for Cancer Immunotherapy. *Front Immunol* 2020;11:589641.
25 D'Alise AM, Brasu N, De Intinis C, *et al*. Adenoviral-based vaccine promotes neoantigen-specific CD8$^+$ T cell stemness and tumor rejection. *Sci Transl Med* 2022;14:eabo7604.
26 D'Alise AM, Leoni G, Cotugno G, *et al*. Phase I Trial of Viral Vector-Based Personalized Vaccination Elicits Robust Neoantigen-Specific Antitumor T-Cell Responses. *Clin Cancer Res* 2024;30:2412–23.